

# Cross-sections for formation of $^{178m^2}\text{Hf}$ and $^{179m^2}\text{Hf}$ through reactions on natural hafnium at neutron energy $14.8 \pm 0.2$ MeV

Junhua Luo · Fei Tuo · Xiangzhong Kong

Received: 8 October 2010 / Published online: 4 January 2011  
© Akadémiai Kiadó, Budapest, Hungary 2011

**Abstract** The cross sections for formation of metastable state of  $^{178}\text{Hf}$  ( $^{178m^2}\text{Hf}$ , 574.215 keV, 31 y) and  $^{179}\text{Hf}$  ( $^{179m^2}\text{Hf}$ , 362.55 keV, 25.05 d) through reactions induced by  $14.8 \pm 0.2$  MeV neutrons on natural hafnium were measured for the first time. The monoenergetic neutron beam was produced via the  $^3\text{H}(\text{d}, \text{n})^4\text{He}$  reaction on ZF-300-II Intense Neutron Generator at Lanzhou University. Induced gamma activities were measured by a gamma-ray spectrometer with high-purity germanium (HPGe) detector. Measurements were corrected for gamma-ray attenuations, random coincidence (pile-up), dead time and fluctuation of neutron flux. The neutron fluence were determined by the cross section of  $^{93}\text{Nb}(\text{n}, 2\text{n})^{92m}\text{Nb}$  reaction. The neutron energy in the measurement were by the cross section ratios of  $^{90}\text{Zr}(\text{n}, 2\text{n})^{89m+g}\text{Zr}$  and  $^{93}\text{Nb}(\text{n}, 2\text{n})^{92m}\text{Nb}$  reactions.

**Keywords** (n, x) Reaction · Cross section · Neutrons · Activation technique · Hafnium

## Introduction

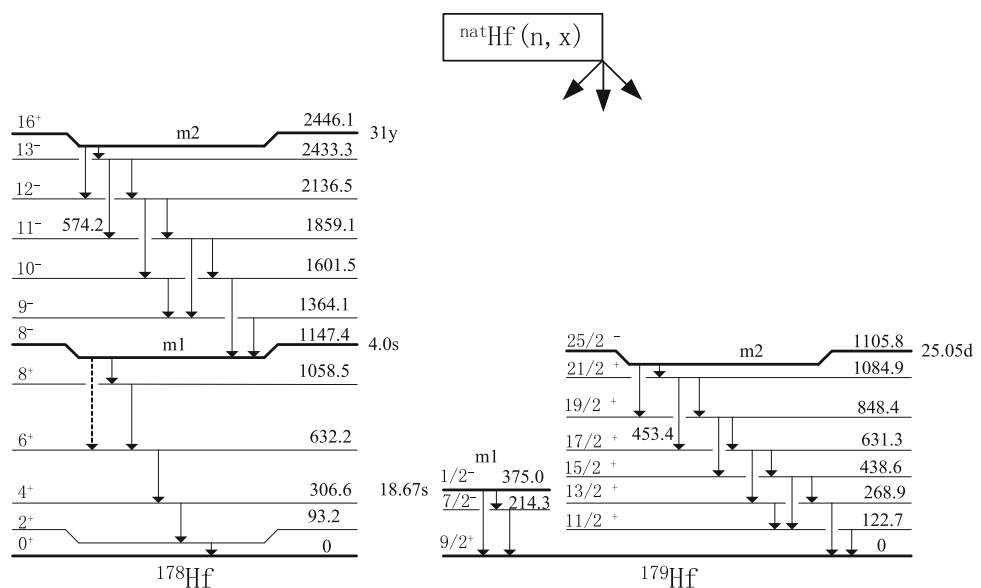
Experimental data of neutron-induced reactions in the energy range around 13 to 15 MeV are needed to verify the accuracy of nuclear models used in the calculation of cross sections. Furthermore, the data are of considerable importance for practical applications, such as for integral calculations on the first wall, blanket and shield of a conceptual fusion power reactor. The data for gas production via neutron induced reactions are of great importance in the domain of fusion reactor technology, particularly of nuclear transmutation rates, nuclear heating and radiation damage due to gas formation. A lot of experimental data on neutron induced cross sections for fusion reactor technology applications have been reported and great efforts have been devoted to compilations and evaluations [1, 2]. In general, cross sections for the formation of isomeric states are more difficult to be predicted than those for the total reaction channels, since more details on the structure of the residual nucleus have to be taken into account (cf. Ref. [3]). The relative probability of forming isomeric states in a nucleus is mainly governed by the spin state values of the levels involved, and the spin distribution of the excited states of the compound nucleus. The high spin value  $16^+$  and  $25/2^-$  of the second isomeric state (m2) of  $^{178}\text{Hf}$  and  $^{179}\text{Hf}$  (Fig. 1) relative to the corresponding values  $0^+$  and  $9/2^+$  of the ground state (g), offers great sensitivity for the study of the spin distribution of the residual nucleus. The cross sections of  $(\text{n}, 2\text{n})$ ,  $(\text{n}, \gamma)$ ,  $(\text{n}, \text{p})$ ,  $(\text{n}, \text{d})$ ,  $(\text{n}, \text{t})$ ... reactions for the isotopes of hafnium have been measured by many authors. Here, we adduced several authors [4–33], but the cross sections of  ${}^{\text{nat}}\text{Hf}(\text{n}, \text{x})^{178m^2}\text{Hf}$  and  ${}^{\text{nat}}\text{Hf}(\text{n}, \text{x})^{179m^2}\text{Hf}$  reactions have been not reported. Most of the authors neglected the effect of  $(\text{n}, \text{n}')$ ,  $(\text{n}, \gamma)$  reactions or deducted the effect indirectly when they calculated the cross section of  $(\text{n}, 2\text{n})$ .

J. Luo  
Department of Physical Science and Electronic Technology,  
Hexi University, Zhangye 734000, Gansu Province,  
People's Republic of China

J. Luo (✉) · X. Kong  
School of Nuclear Science and Technology, Lanzhou University,  
Lanzhou 730000, Gansu Province, People's Republic of China  
e-mail: luojh71@163.com

F. Tuo  
National Institute for Radiological Protection, China CDC,  
Beijing 100088, People's Republic of China

**Fig. 1** Simplified representation of formation and decay of the ground state and isomeric states of  $^{178}\text{Hf}$  [34] and  $^{179}\text{Hf}$  [35]. All energies are in keV



reaction. Thus, we investigate them in order to give the cross section of the element producing certain radioactive product nuclide.

In the present work, the cross-sections of the above mentioned reaction were measured in at neutron energy  $14.8 \pm 0.2$  MeV and a gamma-ray counting technique was applied using gamma-ray spectrometer and data acquisition system. Pure  $\text{HfO}_2$  was used as the target material. The reaction yields were obtained by absolute measurement of the gamma activities of the product nuclei using a coaxial high-purity germanium detector. The neutron energies in this measurement was determined by cross section ratios for the  $^{90}\text{Zr}(n, 2n)^{89\text{m}+g}\text{Zr}$  and  $^{93}\text{Nb}(n, 2n)^{92\text{m}}\text{Nb}$  reactions [36].

## Experimental

Cross sections were measured by activation and identification of the radioactive products. This technique is very suitable for investigating low-yield reaction products and closely space low-lying isomeric states, provided their lifetimes are not too short. The details have been described over the years in many publications [37–41]. Here we give some salient features relevant to the present measurements.

### Samples and irradiations

About 3 g of  $\text{HfO}_2$  powder of natural isotopic composition (>99.95% pure) was pressed at  $10 \text{ ton/cm}^2$ , and a pellet, 0.3 cm thick and 2.0 cm in diameter was obtained. One such pellet was prepared. Monitor foils of Nb (99.999% pure, 0.20 mm thick) of the same diameter as the pellet were then attached in front and at the back of sample.

Irradiation of the samples was carried out at the ZF-300-II Intense Neutron Generator at Lanzhou University and lasted about 22 h with a yield  $\sim 0.8$  to  $2.4 \times 10^{11} \text{ s}^{-1}$ . Neutrons were produced by the  $\text{T(d, n)}^4\text{He}$  reaction with an effective deuteron beam energy of 125 keV and beam current of 20 mA. The tritium-titanium (T-Ti) target used in the generator was  $0.9 \text{ mg/cm}^2$  thick. The neutron fluence rate was monitored by the accompanying alpha-particle so that corrections could be made for small variations in the yield. The accompanying  $\alpha$  particle monitor is shown in Fig. 2. The Au-Si surface barrier detector used in  $135^\circ$  accompanying  $\alpha$ -particle tube was at a distance of 119.7 cm from the target. The groups of samples were placed at  $0^\circ$  angle relative to the beam direction and centered about the T-Ti target at distances of 5 cm. Cross section for  $^{93}\text{Nb}(n, 2n)^{92\text{m}}\text{Nb}$  reaction [42] was selected as monitors to measure the reaction cross section on several Hf isotopes.

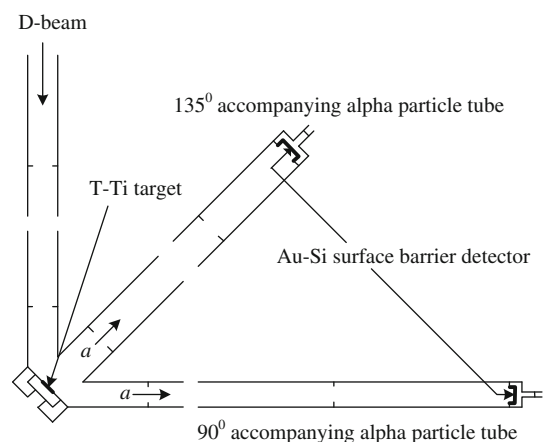


**Fig. 2** ZF-300-II Intense Neutron Generator neutron flux monitor

## Determination of the incident neutron energy

In the D-T reaction ( $Q$  value of 17.6 MeV), induced by deuterons of energy  $E_d$ , the kinetic energy  $E_n$  of the neutrons emitted at angle  $\theta$  can be estimated [43] from the following expression (1);

$$(E_n)^{\frac{1}{2}} = \frac{(M_d M_n E_d)^{\frac{1}{2}} \cos \theta + (M_d M_n E_d \cos^2 \theta + \{M_\alpha + M_n\} [M_\alpha Q + E_d (M_\alpha - M_n)])^{\frac{1}{2}}}{M_\alpha + M_n} \quad (1)$$

where  $M_d$ ,  $M_n$  and  $M_\alpha$  are the masses of deuteron, neutron and alpha particle, respectively. The effective D-T neutron energy at irradiation position was determined by the Nb/Zr method [36, 43–45]. The measured neutron energy was shown in Fig. 3 together with the calculation using Eq. (1). The uncertainty in the neutron energy at  $\sim 5$  cm was estimated to be 200 keV from a consideration of the sample sizes,  $d^+$  beam diameter of about 3–4 mm, and the uncertainty in the Nb/Zr method [36].

The neutron energies were obtained both by the Eq. (1) and the Nb/Zr method (Lewis and Zieba [36]). The results are shown in Fig. 3. It can be seen, measured result is somewhat lower than the calculated value at neutron energy of 14.8 MeV. This discrepancy is probably due to the samples corresponding to the solid angle geometry, the neutron transport and scattering processes in the target and integrates over the sample volume. But measured result is consistent with the calculated value of Eq. (1) within the experimental uncertainty.

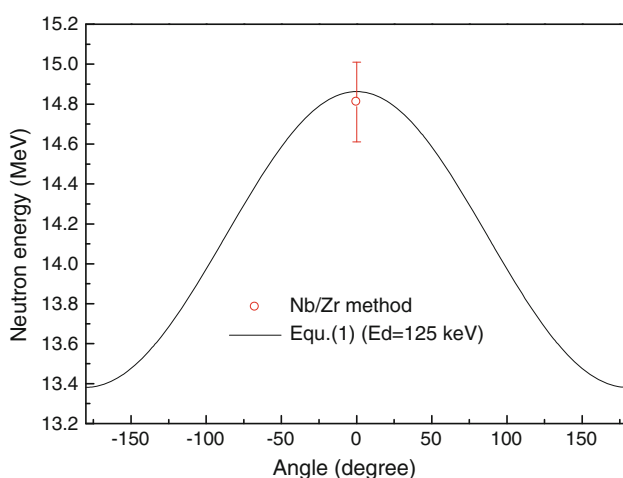


**Fig. 3** Angular dependence of d-T neutron energy. The neutron energies were calculated by choosing the incident deuteron energy  $E_d = 125$  keV. The open circle show experimental data determined by the Nb/Zr method (Lewis and Zieba, [36])

## Measurement of radioactivity

The gamma ray activity of  $^{178m^2}\text{Hf}$ ,  $^{179m^2}\text{Hf}$ , and  $^{92m}\text{Nb}$  was determined by a CH8403 coaxial high-purity germanium detector made in the People's Republic of China with a relative efficiency of 20% and an energy resolution of 3 keV at

1332 keV. The efficiency of the detector was calibrated using the standard gamma source, Standard Reference Material 4275 from the National Institute of Standards and Technology, Washington, D.C., USA. An absolute efficiency calibration curve was obtained at 20 cm from the surface of the germanium crystal. At this distance the coincidence losses can be considered to be negligible. In our case, however, we needed to calibrate the efficiency at 2 cm, the actual counting position used because of the weak activity of the sample. Therefore, we selected a set of single  $\gamma$ -line sources ( $^{137}\text{Cs}$ ,  $^{54}\text{Mn}$ ) and placed them at two positions (20 and 2 cm) successively to measure their efficiency ratios to be able to evaluate the efficiency ratio curve as a function of energy. The absolute efficiency calibration curve at 2 cm was obtained from the calibration curve at 20 cm and the efficiency ratio curve. The uncertainty in the absolute efficiency curve at 2 cm was estimated to be  $\sim 2\text{--}3\%$ , while the uncertainty of the activity of the standard source is  $\sim 1.0\%$ .

The decay characteristics of the product radioisotopes and the natural abundances of the target isotopes under investigation are summarized in Table 1, [34, 35, 46].

## Calculation of cross sections and their uncertainties

The measured cross sections can be calculated by the following formula [cf. 47]:

$$\sigma_x = \frac{[SeI_\gamma K\eta MD]_m [\lambda AFC]_x}{[SeI_\gamma K\eta MD]_x [\lambda AFC]_m} \sigma_m \quad (2)$$

where the subscript  $m$  represents the term corresponding to the monitor reaction and subscript  $x$  corresponds to the measured reaction,  $\varepsilon$  full-energy peak efficiency of the measured characteristic gamma-ray,  $I_\gamma$  gamma-ray intensity,  $\eta$  abundance of the target nuclide,  $M$  mass of sample,  $D = e^{-\lambda t_1} - e^{-\lambda t_2}$  counting collection factor,  $t_1, t_2$  time intervals from the end of the irradiation to the start and end of counting, respectively,  $A$  atomic weight,  $C$  measured full energy peak area,  $\lambda$  decay constant,  $F$  total correction factor of the activity:

**Table 1** Reactions and associated decay data of activation products

Reaction	Abundance of target isotope (%)	Mode of decay (%)	Half-life of product	$E\gamma$ (keV)	$I\gamma$ (%)	Reference
$^{nat}Hf(n, x)^{178m^2}Hf$	100	IT (100)	31 y	574.219	89.9	[34]
$^{nat}Hf(n, x)^{179m^2}Hf$	100	IT (100)	25.05 d	362.55	41.1	[35]
$^{93}Nb(n, 2n)^{92m}Nb$	100	EC (100)	10.15 d	934.4	99.07	[46]

$$F = f_s \times f_c \times f_g \quad (3)$$

where  $f_s$ ,  $f_c$  and  $f_g$  are correction factors for the self-absorption of the sample at a given gamma-energy, the coincidence sum effect of cascade gamma-rays in the investigated nuclide and in the counting geometry, respectively. Coincidence summing correction factor  $f_c$  was calculated by the method [48]. In turn, the gamma ray attenuation correction factors  $f_s$  in the  $HfO_2$  foil and the geometry correction  $f_g$  were calculated by the following Eqs. (4) and (5), respectively.

$$f_s = \frac{\mu h}{1 - \exp(-\mu h)} \quad (4)$$

$$f_g = \frac{(D + h/2)^2}{D^2} \quad (5)$$

Here  $\mu$  (in  $cm^{-1}$ ) is the linear attenuation coefficient in  $HfO_2$  for gamma rays at each of the photon energies  $E$ ,  $h$  (in cm) the thickness of the sample and  $D$  is the distance from the measured sample to the surface of the germanium crystal.

$K$  neutron fluence fluctuation factor:

$$K = \left[ \sum_i^L \Phi_i (1 - e^{-\lambda \Delta t_i}) e^{-\lambda T_i} \right] / \Phi S \quad (6)$$

where  $L$  number of time intervals into which the irradiation time is divided,  $\Delta t_i$  duration of the  $i$ th time interval,  $T_i$  time interval from the end of the  $i$ th interval to the end of irradiation,  $\Phi_i$  neutron flux averaged over the sample during  $\Delta t_i$ ,  $S = 1 - e^{-\lambda T}$  growth factor of the product nuclide,  $T$  total irradiation time,  $\Phi$  neutron flux averaged over the sample during the total irradiation time  $T$ .

One can easily derive the expression of the Eq. (1)  $\eta_x \sigma_x$  as

$$\eta_x \sigma_x = \frac{[SeI_\gamma \eta KMD]_m [\lambda AFC]_x}{[SeI_\gamma KMD]_x [\lambda AFC]_m} \sigma_m \quad (7)$$

Since the samples we selected are natural abundance, furthermore, the hafnium has many isotopes ( $^{174}Hf$ , 0.162%;  $^{176}Hf$ , 5.206%;  $^{177}Hf$ , 18.606%;  $^{178}Hf$ , 27.297%;  $^{179}Hf$ , 13.629%;  $^{180}Hf$ , 35.100%) [46], it is obvious that a radioactive nuclide can be produced by several reactions, such as the reaction  $^{nat}Hf(n, x)^{178m^2}Hf$  is made up of

$^{179}Hf(n, 2n)^{178m^2}Hf$ ,  $^{178}Hf(n, n')^{178m^2}Hf$ ,  $^{177}Hf(n, \gamma)^{178m^2}Hf$ ,  $^{178m^2}Hf$ ,  $^{nat}Hf(n, x)^{179m^2}Hf$  is made up of  $^{180}Hf(n, 2n)^{179m^2}Hf$ ,  $^{179m^2}Hf$ ,  $^{179}Hf(n, n')^{179m^2}Hf$ ,  $^{178}Hf(n, \gamma)^{179m^2}Hf$  and so on. Surely, each of the reactions producing certain radioactive product has different contribution. So in the calculation we just gave the cross section of the element and didn't import the abundance of the target nuclide into the formula. For the reaction  $^{nat}Hf(n, x)^{178m^2}Hf$ , there are three routes to produce  $^{178m^2}Hf$ , the first via the  $^{179}Hf(n, 2n)^{178m^2}Hf$  reaction, the second through the  $^{178}Hf(n, n')^{178m^2}Hf$  reaction, and the third via  $^{177}Hf(n, \gamma)^{178m^2}Hf$  reaction. So the cross section of  $^{nat}Hf(n, x)^{178m^2}Hf$  reaction can be calculated by the following formula:

$$\begin{aligned} \sigma(^{nat}Hf(n, x)^{178m^2}Hf) &= 0.13629 \sigma(^{179}Hf(n, 2n)^{178m^2}Hf) \\ &+ 0.27297 \sigma(^{178}Hf(n, n')^{178m^2}Hf) \\ &+ 0.18606 \sigma(^{177}Hf(n, \gamma)^{178m^2}Hf) \\ &= \frac{[SeI_\gamma \eta KMD]_m [\lambda AFC]_x}{[SeI_\gamma KMD]_x [\lambda AFC]_m} \sigma_m \end{aligned} \quad (8)$$

For the reaction  $^{nat}Hf(n, x)^{179m^2}Hf$ , there are three routes to produce  $^{179m^2}Hf$ , the first via the  $^{180}Hf(n, 2n)^{179m^2}Hf$  reaction, the second through the  $^{179}Hf(n, n')^{179m^2}Hf$  reaction, and the third via  $^{178}Hf(n, \gamma)^{179m^2}Hf$  reaction. So the cross section of  $^{nat}Hf(n, x)^{179m^2}Hf$  reaction can be calculated by the following formula:

$$\begin{aligned} \sigma(^{nat}Hf(n, x)^{179m^2}Hf) &= 0.35100 \sigma(^{180}Hf(n, 2n)^{179m^2}Hf) \\ &+ 0.13629 \sigma(^{179}Hf(n, n')^{179m^2}Hf) \\ &+ 0.27297 \sigma(^{178}Hf(n, \gamma)^{179m^2}Hf) \\ &= \frac{[SeI_\gamma \eta KMD]_m [\lambda AFC]_x}{[SeI_\gamma KMD]_x [\lambda AFC]_m} \sigma_m \end{aligned} \quad (9)$$

The main contributions to the uncertainty of measurement in our work result from counting statistics (0.1–15%), standard cross sections uncertainties (1%), detector efficiency (2–3%), weight of samples (0.1%), self-absorption of gamma-ray (0.5%) and the coincidence sum effect of cascade gamma-rays (0–5%), the uncertainties of irradiation, cooling and measuring times (0.1–1%), etc. And some other uncertainty contribution form the parameters of the measured nuclei and standard nuclei, such

as, uncertainties of the branching ratio of the characteristic gamma rays, uncertainties of the half life of the radioactive product nuclei and so on all are considered.

## Results and conclusions

### Results

Using the relative activation technique of neutron, the sample was sandwiched between two Nb foils which were used as monitor. Because the cross section of  $^{93}\text{Nb}(n, 2n)^{92m}\text{Nb}$  reaction has been measured by many authors, we can select it as a standard. With the irradiation taking place, the neutron flux for the sample was the same as the flux for the monitors. So we can find an equation of neutron flux between them, and avoid importing the neutron flux into the calculation.

After having been irradiated, the samples were cooled for 5–24 days, and one sample was measured with a 20% relative efficiency HPGe detector. One of the gamma-ray spectra is shown in Fig. 4. Cross-section values for  $^{nat}\text{Hf}(n, x)^{178m^2}\text{Hf}$  and  $^{nat}\text{Hf}(n, x)^{179m^2}\text{Hf}$  reactions were obtained relative to those of the  $^{93}\text{Nb}(n, 2n)^{92m}\text{Nb}$  reaction. The cross sections for the  $^{93}\text{Nb}(n, 2n)^{92m}\text{Nb}$  reaction, which is  $459.7 \pm 5.0$  mb at  $14.8 \pm 0.2$  MeV incident neutron energies, was obtained by interpolating the evaluated values of the literature [42]. The cross-sections measured in the present work are summarized in Table 2.

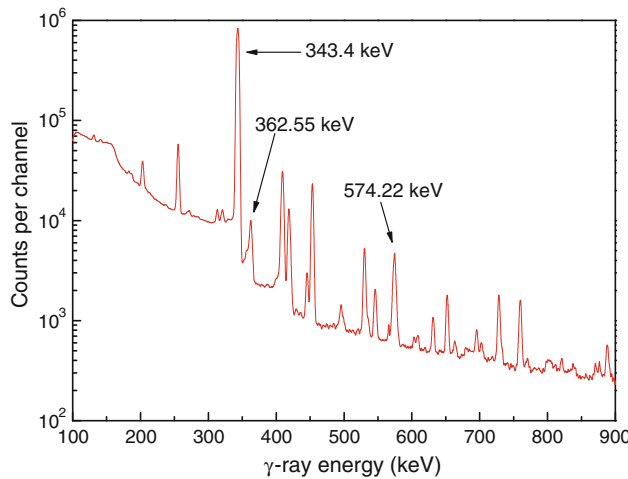


**Fig. 4** The  $\gamma$ -ray spectra of about 24 days after the end of irradiation

**Table 2** Summary of cross-section measurements

Reaction	Cross-sections (mb) at neutron energy $14.8 \pm 0.2$ (MeV)	Expanded standard uncertainty	Coverage factor k
$^{nat}\text{Hf}(n, x)^{178m^2}\text{Hf}$	7.2	3.0	2
$^{nat}\text{Hf}(n, x)^{179m^2}\text{Hf}$	18.6	3.4	2

## Conclusions

We have measured the activation cross sections for  $^{nat}\text{Hf}(n, x)^{178m^2}\text{Hf}$  and  $^{nat}\text{Hf}(n, x)^{179m^2}\text{Hf}$  reactions on hafnium isotopes induced by  $14.8 \pm 0.2$  MeV neutrons. It should be mentioned that this work presents the first cross-sections for formation of  $^{178m^2}\text{Hf}$  and  $^{179m^2}\text{Hf}$  through reactions on natural hafnium. The high precision of the cross-sections obtained in the earlier measurement was limited, because there are  $^{174}\text{Hf}$ ,  $^{176}\text{Hf}$ ,  $^{177}\text{Hf}$ ,  $^{178}\text{Hf}$ ,  $^{179}\text{Hf}$ , and  $^{180}\text{Hf}$  isotopes in the natural hafnium and overlapping of the gamma-peaks from different isotopes could not be neglected in the gamma-spectrum measurements with the use of NaI(Tl) detectors. The decay data such as half-life and branching ratio of the radioactive product nuclei were imprecise at that early time. In recent years, the reliabilities of the results have improved with the use of the Ge semiconductor detectors and the more accurate above-mentioned parameters. A good plan of irradiation and cooling time is also important and in our experiment we selected different irradiation time according to the half-life of the product nuclei. In addition, the present measurements were performed in the Low Background Laboratory of Lanzhou University and disturbance from environmental radiation was reduced to a very low level. In conclusion, our data would improve the quality of the neutron cross-section database.

**Acknowledgments** We would like to thank the Intense Neutron Generator group at Lanzhou University for performing the irradiations. This work was supported by the Program for Long Yuan Young Innovative Talents of Gansu Province, China and Scientific Research Start up Outlay of High-Position Talent in Hexi University in Gansu Province, China.

## References

1. CINDA-A (2000) The index to literature and computer files on microscopic neutron data. International Atomic Energy Agency, Vienna
2. McLane V, Dunford CL, Rose PF (1988) Neutron cross sections, vol 2. Academic, New York
3. Qaim SM, Mushtaq A, Uhl M (1988) Phys Rev C 38:645
4. Hillman M, Shikata E (1969) Cross sections of some reactions of hafnium isotopes with 14.5 MeV neutrons. J Inorg Nucl Chem 31:909
5. Qaim SM (1974) Total (n, 2n) cross sections and isomeric cross-section ratios at 14.7 MeV in the region of rare earths. Nucl Phys A 224:319

6. Lakshmana Das N, Srinivasa Rao CV, Rama Rao J (1981) Some neutron activation cross-sections in the heavy mass region. *Ann Nucl Energy* 8:283
7. Kong X, Wang Y, Yang J (1998) Cross sections for (n, 2n), (n, p) and (n,  $\alpha$ ) reactions on rare-earth isotopes at 14.7 MeV. *Appl Radiat Isot* 49:1529
8. Meadows JW, Smith DL, Greenwood LR, Haight RC, Ikeda Y, Konno C (1996) Measurement of fast-neutron activation cross sections for copper, europium, hafnium, iron, nickel, silver, terbium and titanium at 10.0 and 14.7 MeV and for the Be(d, n) thick-target spectrum. *Ann Nucl Energy* 23:877
9. Lakshmana Das N, Srinivasa Rao CV, Thirumala Rao BV, Rama Rao J (1974) Pre-compound decay in (n, 2n) reactions at 14.2 MeV. *Nucl Solid State Phys Symp* 2:105
10. Kiraly B, Csikai J, Doczi R (2001) Validation of neutron data libraries by differential and integral cross sections, JAERI Conference Proceedings, 283
11. Doczi R, Semkova V, Fenyesi A, Yamamoto N, CsM Buczko, Csikai J (1998) Excitation functions of some (n, p) and (n,  $\alpha$ ) reactions from threshold to 16 MeV. *Nucl Sci Eng* 129:164
12. Djumin AN, Egorov AI, Lebedev VM, Popova GN, Smolin VA (1977) Nuclear radii for some isotopes derived from total neutron cross-sections, All Union Conference on Neutron Physics, Kiev, 18–22 Apr 2:74
13. Goryachev AM, Zalesnyi GN (1977) Giant dipole resonance in Hf isotopes. *Yad Fiz* 26:465
14. Salaita GN, Eapen DK (1973) Production cross sections of isomers in As, Y, In, and Hf with 14.8 MeV neutrons. *Trans Am Nucl Soc* 16:59
15. Meason JL, Ganapathy R, Kuroda PK (1966) 14.8 MeV neutron activation cross sections for  $^{181}\text{Ta}(n, \alpha)$   $^{178}\text{m}$ , gLu and  $^{178}\text{Hf}(n, p)$   $^{178}\text{m}$ , gLu. *Radiochim Acta* 6:26
16. Coleman RF, Hawker BE, O'connor LP, Perkin JL (1959) Cross sections for (n,p) and (n, $\alpha$ ) reactions with 14.5 MeV neutrons, Proceedings of the Physical Society (London) 73:215
17. Konno C, Ikeda Y, Nakamura T (1990) Activation cross section measurements at neutron energy from 13.3 MeV to 15.0 MeV for  $^{84}\text{Sr}$ ,  $^{113}\text{In}$ ,  $^{115}\text{In}$ ,  $^{178}\text{Hf}$ ,  $^{179}\text{Hf}$  and  $^{180}\text{Hf}$ , Japanese Report to NEANDC 15:155
18. Murahira S, Satoh Y, Honda N, Takahashi A, Iida T, Shibata M, Yamamoto H, Kawade K (1995) Measurement of formation cross sections producing short-lived nuclei by 14 MeV neutrons—Pr, Ba, Ce, Sm, W, Sn, Hf, Japanese Report to the I.N.D.C., 171, 175/U
19. Konno C, Ikeda Y, Oishi K, Kawade K, Yamamoto H, Maekawa H (1993) Activation cross section measurements at neutron energy from 13.3 to 14.9 MeV, JAERI Reports, 1329
20. Ikeda Y, Konno C, Kumar A, Kasugai Y (1996) Summary of activation cross sections measurements at fusion neutron source in jaeri, IAEA Nuclear Data Section Report to the I.N.D.C., 19:342
21. Kirov A, Nenoff N, Georgieva E, Necheva C, Ephtimov I (1993) Activation cross sections and isomeric ratios in reactions induced by 14.5 MeV neutrons in Sm-152, Sm-154 and Hf-178. *Zeitschrift fuer Physik A* 245:285
22. Gurevich GM, Lazareva LE, Mazur VM, SYu Merkulov, Solodukhov GV (1980) Total photoabsorption cross sections for high-z elements in the energy range 7–20 MeV. *Nucl Phys A* 338:97
23. Goryachev BI, Kuznetsov YV, Orlin VN, Pozhidaeva NA, Shevchenko VG (1976) Giant resonance in the strongly deformed nuclei  $^{159}\text{Tb}$ ,  $^{165}\text{Ho}$ ,  $^{166}\text{Er}$ , and  $^{178}\text{Hf}$ . *Yad Fiz* 23:1145
24. Gurevich GM, Lazareva LE, Mazur VM, SYu Merkulov, Solodukhov GV, Tyutin VA (1981) Total nuclear photoabsorption cross sections in the region  $150 < A < 190$ . *Nucl Phys A* 351:257
25. Ikeda Y, Smith DL, Kumar A, Konno C (1991) Measurements of long-lived activation cross sections by 14 MeV neutrons at FNS, JAERI-M Reports, 272
26. Sakane H, Kasugai Y, Shibata M, Iida T, Takahashi A, Fukahori T, Kawade K (2002) Measurement of activation cross section of (n, np + d) reactions producing short-lived nuclei in the energy range between 13.4 and 14.9 MeV using an intense neutron source Oktavian. *Ann Nucl Energy* 29:53
27. Prasad R, Sarkar DC, Khurana CS (1966) Measurement of (n, 2n) reaction cross sections at 14.8 MeV. *Nucl Phys* 88:349
28. Kong X, Wang Y, Yang J, Yuan J (1995) Recent progress on 14 MeV neutron activation cross section measurements. *Communication of Nuclear Data Progress* 14:5
29. Yu W, Lu H, Zhao W (1992) Measurement of activation cross section for  $\text{Hf-179}(n, 2n)\text{Hf-178m}_2$  reaction. *Chin J Nucl Phys* 14:326 (Beijing)
30. Kasugai Y, Yamamoto H, Kawade K, Ikeda Y, Uno Y, Maekawa H (1994) Activation cross section measurement of reactions producing short-lived nuclei at neutron energy between 13.4 MeV and 14.9 MeV, Conference on Nuclear Data for Science and Technology, Gatlinburg 935
31. Rurarz E, Haratym Z, Pietrzykowski M, Sulik A (1970) Excitation of short-living isomeric activities with 14.5 MeV neutrons. *Acta Phys Polonica* B1:415
32. Gurevich GM, Lazareva LE, Mazur VM, Solodukhov GV (1976) About the width of giant resonance in the g-quanta absorption cross sections in the range of nuclei with  $A = 150\text{--}200$ . *Zhurnal Eksper i Teoret Fiz Pisma v Redakt* 23:411
33. Demekhina NA, Danagulyan AS, Karapetyan GS (2001) Remarks to the problem of the isomeric state production in the ( $\gamma, \gamma'$ ) reactions in the giant dipole resonance. *Yad Fiz* 64:1879
34. Achterberg E, Capurro OA, Marti GV (2009) Nuclear data sheets for  $A = 178$ . *Nucl Data Sheets* 110:1473–1688
35. Coral M, Baglin (2009) Nuclear data sheets for  $A = 179$ . *Nucl Data Sheets* 110:265–506
36. Lewis VE, Zieba KJ (1980) A transfer standard for d + T neutron fluence and energy. *Nucl Instr Meth* 174:141
37. Luo J, Liu G, Tuo F, Kong X, Liu R, Li J, Lou B (2007) *Phys Rev C* 76:057601
38. Luo J, Wang X, Liu Z, Tuo F, Kong X (2010) *Radiat Phys chem* 79(10):1018–1021
39. Bostan M, Qaim SM (1994) *Phys Rev C* 49:266
40. Cserpák F, Sudár S, Csika J, Qaim SM (1994) *Phys Rev C* 49:1525
41. Nesaraja CD, Sudár S, Qaim SM (2003) *Phys Rev C* 68:024603
42. Wagner M, Vonach H, Pavlik A, Strohmaier B, Tagesen S, Martinez-Rico J (1990) Physik daten-physics data, evaluation of cross sections for 14 important neutron-dosimetry reactions, fachinformationszentrum karlsruhe, Gesellschaft für wissenschaftlich-technische Information mbH, in the Federal Republic of Germany. No. 13–5
43. Curtis LF (1969) Introduction to neutron physics. D. Van Nostrand Company, Princeton
44. Nethaway DR (1978) *J Inorg Nucl Chem* 40:1285
45. Pavlik A, Winkler H, Vonach H, Paulsen A, Liskin H (1982) *J Phys G Nucl Phys* 8:1283
46. Browne E, Firestone RB (1996) Table of isotopes. Wiley, New York
47. Luo Junhua, Chenghu Li, Liu Zhenlai, Wang Xinxing, Liu Rong, Jiang Li (2010) *J Radioanal Nucl Chem* V283(2):421–426
48. Mc GrahamJ, Co GraemeE (1975) *Nucl Instr Meth* 130:189–197